

Ascorbate and Iron Are Required for the Specification and Long-Term Self-Renewal of Human Skeletal Mesenchymal Stromal Cells

Tong Ming Liu,^{1,2,3,*} Ege Deniz Yildirim,¹ Pin Li,¹ Hai Tong Fang,⁴ Vinitha Denslin,^{5,10} Vibhor Kumar,⁶ Yui Han Loh,⁴ Eng Hin Lee,^{5,10} Simon M. Cool,³ Bin Tean Teh,² James H. Hui,^{5,10} Bing Lim,¹ and Ng Shyh-Chang^{7,8,9,*}

¹Cancer Stem Cell Group, Genome Institute of Singapore, Agency for Science, Technology and Research (A*STAR), 60 Biopolis Street, Singapore 138672, Singapore

²Institute of Molecular and Cell Biology, Agency for Science Technology and Research, Singapore 138673, Singapore

³Glycotherapeutics Group, Institute of Medical Biology, Agency for Science Technology and Research, Singapore 138648, Singapore

⁴Epigenetics and Cell Fates Laboratory, Institute of Molecular and Cell Biology, Agency for Science Technology and Research, Singapore 138673, Singapore

⁵Department of Orthopaedic Surgery, National University of Singapore, Lower Kent Ridge Road, Singapore 119260, Singapore

⁶Computational and Systems Biology Group, Genome Institute of Singapore, A*STAR, Singapore 138672, Singapore

⁷State Key Laboratory of Stem Cell and Reproductive Biology, Institute of Zoology, Chinese Academy of Sciences, 1 Beichen West Road, Chaoyang District, Beijing 100101, China

⁸Institute of Stem Cell and Regeneration, Chinese Academy of Sciences, Beijing, China

⁹University of Chinese Academy of Sciences, Beijing, China

¹⁰NUS Tissue Engineering Program, Life Sciences Institute, National University of Singapore, Lower Kent Ridge Road, Singapore 119260, Singapore

*Correspondence: dbsliutm@yahoo.com (T.M.L.), huangsq@ioz.ac.cn (N.S.-C.)

<https://doi.org/10.1016/j.stemcr.2020.01.002>

SUMMARY

The effects of ascorbate on adult cell fate specification remain largely unknown. Using our stepwise and chemically defined system to derive lateral mesoderm progenitors from human pluripotent stem cells (hPSCs), we found that ascorbate increased the expression of mesenchymal stromal cell (MSC) markers, purity of MSCs, the long-term self-renewal and osteochondrogenic capacity of hPSC-MSCs *in vitro*. Moreover, ascorbate promoted MSC specification in an iron-dependent fashion, but not in a redox-dependent manner. Further studies revealed that iron synergized with ascorbate to regulate hPSC-MSC histone methylation, promote their long-term self-renewal, and increase their osteochondrogenic capacity. We found that one of the histone demethylases affected by ascorbate, KDM4B, was necessary to promote the specification of hPSC-MSCs. This mechanistic understanding led to the metabolic optimization of hPSC-MSCs with an extended lifespan *in vitro* and the ability to fully repair cartilage defects upon transplantation *in vivo*. Our results highlight the importance of ascorbate and iron metabolism in adult human cell fate specification.

INTRODUCTION

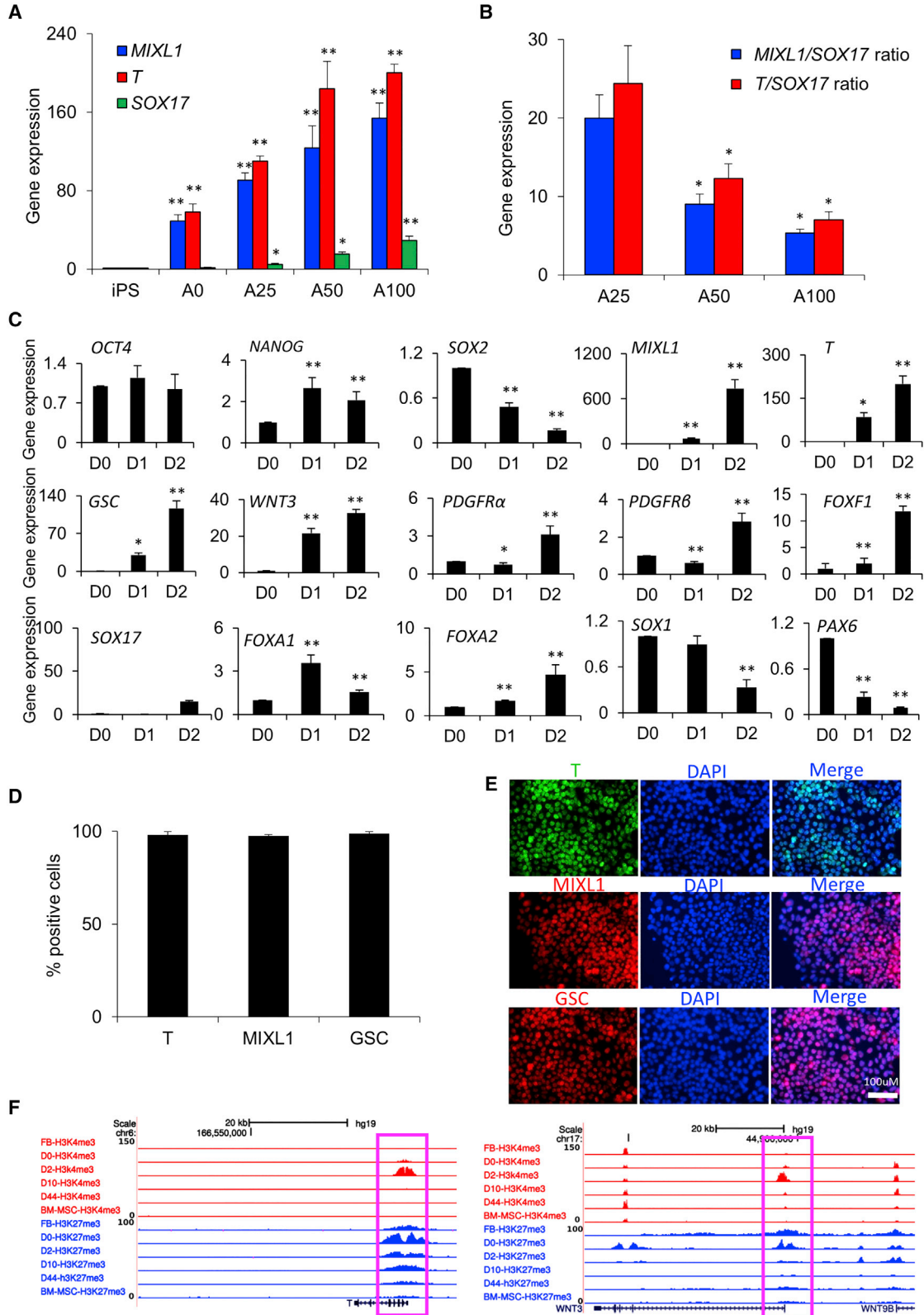
Ascorbate, or vitamin C, is an important cofactor for many biochemical reactions in the human body, and thus exerts pleiotropic effects in stem cell biology. For example, ascorbate can function as a potent antioxidant, a cofactor for dioxygenases, and a cofactor for collagen synthesis. Although the effects of ascorbate on induced pluripotent stem cell (iPSC) reprogramming and on iPSCs are well known (Chen et al., 2013; Chung et al., 2010; Wang et al., 2011), its effects on adult cell fate specification have been less clear.

Embryonic mesoderm progenitors, under the influence of a multitude of developmental signaling pathways, produce the long bones in the adult limbs, which also harbor adult skeletal mesenchymal stromal cells (MSCs) (Alman, 2015; Prockop, 2009). During embryonic development, all cartilage, bone, and bone marrow in the limbs and the appendicular skeleton originate from the lateral plate mesoderm. Adult skeletal MSCs are capable of multi-lineage differentiation into cartilage, bone, and adipose tissues. However, both scientific and clinical studies of MSCs have been hampered by their poor retention of differentiation

potential and self-renewal capacity during long-term culture *in vitro*. Although there are reports of MSCs derived from the infinitely self-renewing human pluripotent stem cells (hPSCs) (Barberi et al., 2005; Hwang et al., 2008; Olivier et al., 2006; Vodnyanik et al., 2010), their use of non-defined components, such as fetal bovine serum or OP9 feeder cells, greatly compromise their consistency and clinical applicability. Current differentiation protocols of iPSCs into MSCs are also not efficient, often requiring cell sorting. Thus, there is a need to establish a chemically defined platform to fully recapitulate each major phase of MSC development efficiently. Such a platform would also be useful to test the roles of ascorbate and other small molecules during skeletal MSC specification and long-term self-renewal.

In this study, we developed a platform to fully recapitulate the major phases of MSC development *in vitro*. This *in vitro* platform involves three phases, including the induction of primitive streak cells, differentiation into lateral mesoderm progenitors, and specification of MSCs. This platform provides intermediate cells, previously inaccessible in human embryos, that represent the different phases of MSC development. In the process, we found that ascorbate increased the





(legend on next page)



expression of MSC markers by transcriptomic profiling, increased the purity of MSCs by surface antigen profiling, and increased the self-renewal and osteochondrogenic capacity of hPSC-MSCs. Moreover, ascorbate promoted MSC specification in an iron-dependent fashion, but not in a redox-dependent manner. Further studies revealed that iron synergized with ascorbate to regulate histone methylation in hPSC-MSCs, promote their self-renewal and increase their osteochondrogenic capacity. Furthermore, our results suggest that one of the JmjC histone demethylases affected by ascorbate, KDM4B, is necessary and sufficient to promote specification of lateral mesoderm progenitors into human MSCs. This mechanistic understanding led to the derivation of human MSCs with an extended lifespan and enhanced osteochondrogenic potential. Furthermore, our hPSC-MSCs can fully repair cartilage defects upon transplantation *in vivo*. These results highlight the importance of ascorbate and iron metabolism in adult stem cell fate specification and long-term self-renewal, with important implications for tackling human stem cell aging (Li et al., 2016; Zhang et al., 2015).

RESULTS

Optimal Activin and Wnt Synergism for Complete Induction of Primitive Streak Cells

iPSCs were generated from MRC5 human embryonic lung fibroblasts or BJ foreskin fibroblasts (Figure S1) (Takahashi et al., 2007). Activin A is known to be essential to induce primitive streak cells from PSCs (Gadue et al., 2006; Nostro et al., 2008). Our results showed that activin A enhanced induction into primitive streak cells expressing the key transcription factors (TFs): *T* (Brachyury) and *MIXL1* (Figure 1A). However, the endodermal TF *SOX17* was also increased with increasing doses of activin A. We found that the ratio of *MIXL1* (or *T*) to *SOX17* was the highest when we optimized the dose at 25 ng/mL of activin A (Figure 1B). Wnt signaling is also essential for inducing primitive streak cells from PSCs

(Gadue et al., 2006; Liu et al., 1999). CHIR99021, a GSK3 β inhibitor, is known to activate canonical Wnt signaling by stabilizing β -catenin. Our data showed that activin A and CHIR99021 synergistically promoted primitive streak induction. Compared to Wnt3a, CHIR99021 was superior in promoting cell adherence (Figure S2A), as well as induction of the primitive streak TFs: *MIXL1*, *T* (Brachyury), and *GSC* (Figure S2B). Although addition of fibroblast growth factor 2 (FGF2) at day 2 did not further enhance primitive streak induction, expression of mesoderm TFs, such as *HAND1* and *FOXF1* increased in the presence of FGF2 (Figure S2B).

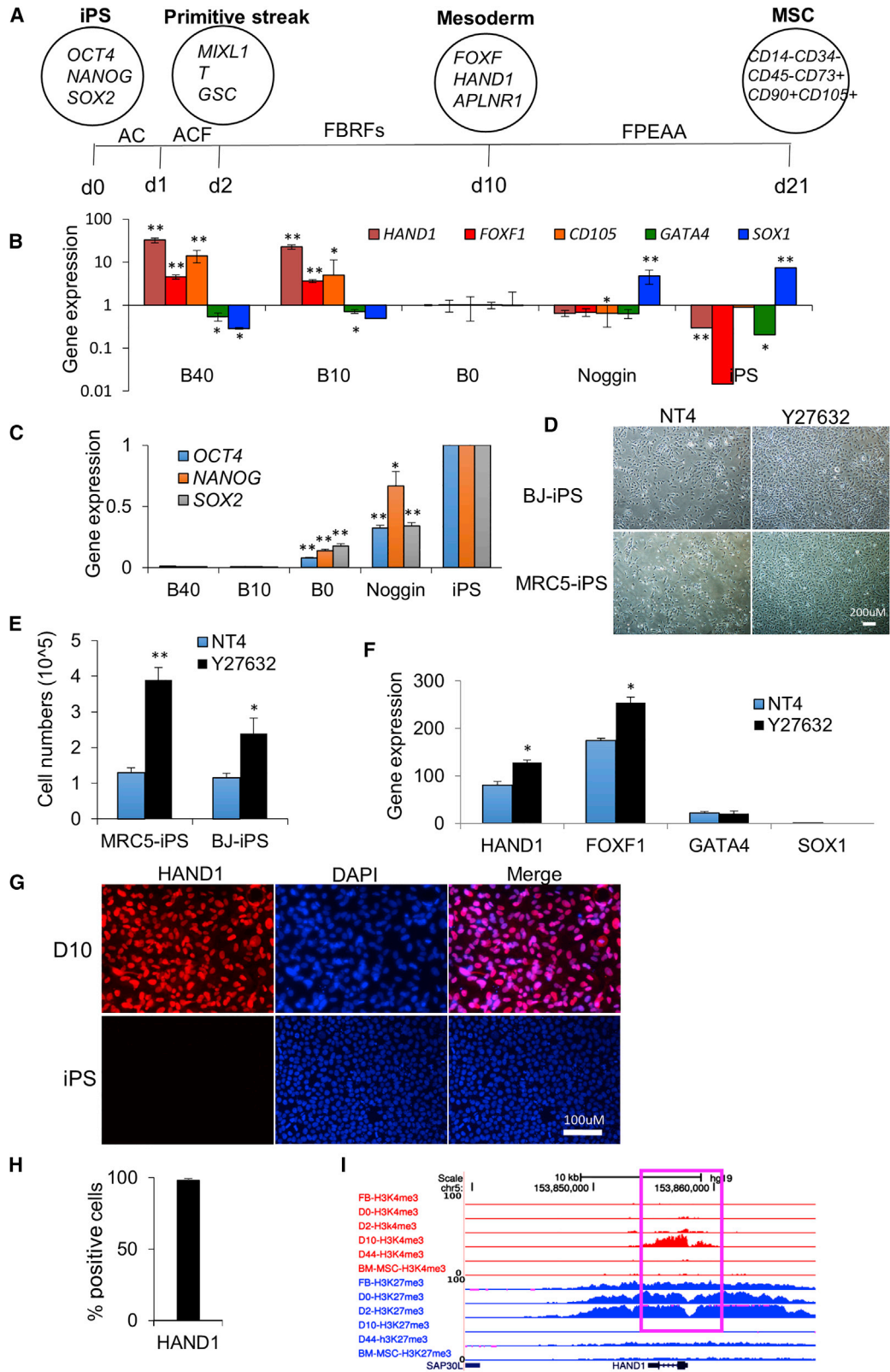
Thus, in phase 1 (D0-2) of our platform (Figure S2A), i.e., primitive streak induction, *SOX2* significantly decreased, while the primitive streak TFs *T* (Brachyury), *MIXL1*, and *GSC* peaked at day 2 (Figures 1C and S3). Fluorescence-activated cell sorting (FACS) showed that our protocol yielded 98.13% \pm 1.7% T+, 97.53% \pm 0.7% MIXL1+, and 98.77% \pm 1.13% GSC+ cells (Figure 1D). Immunofluorescence staining confirmed the qRT-PCR and FACS data (Figure 1E). Several mesoderm markers, such as *WNT3*, *PDGFR α* , *PDGFR β* , *HAND1*, and *FOXF1* were also upregulated. In contrast, endodermal TFs, such as *SOX17*, *FOXA1*, *FOXA2*, and ectodermal TFs, such as *SOX1* and *PAX6* were either downregulated or remained low in expression (Figures 1C, S2B, and S3). Genome-wide epigenetic patterns were consistent with gene expression. Chromatin immunoprecipitation sequencing (ChIP-seq) for methylation of histone H3 Lys 4 (H3K4me3) and H3 Lys 27 (H3K27me3), chromatin markers of active and repressed promoters, respectively, showed that the *T* (Brachyury) and *WNT3* promoters were specifically active only at day 2 (Figure 1F). These data demonstrated that hPSCs were efficiently induced into primitive streak cells at day 2.

Lateral Mesoderm Progenitors Require BMP4 Signaling and ROCK Inhibition

In phase 2 (D3-10, Figure 2A) of our platform, we aimed at differentiation into lateral mesoderm progenitors, which

Figure 1. Induction of Primitive Streak Cells from Human Pluripotent Stem Cells

- (A) Titration of activin A (0, 25, 50, and 100 ng/mL) against primitive streak induction, as determined by qRT-PCR for *MIXL1*, *T* (Brachyury), and *SOX17* on day 2. Data are represented as mean \pm SD, n = 3 independent experiments. *p < 0.05, **p < 0.01.
- (B) Optimization of activin A for primitive streak induction, based on the ratio of the primitive streak TFs *MIXL1*, or *T* (Brachyury), to the endodermal TF *SOX17* (compared with activin A, 25 ng/mL). Data are represented as mean \pm SD, n = 3 independent experiments. *p < 0.05.
- (C) qRT-PCR for pluripotency TFs (*OCT4*, *NANOG*, *SOX2*), primitive streak TFs (*MIXL1*, *T*, *GSC*), mesodermal markers (*WNT3*, *PDGFR α/β* , *FOXF1*), endodermal TFs (*SOX17*, *FOXA1*, *FOXA2*), and ectodermal TFs (*SOX1*, *PAX6*) during phase 1, or the primitive streak induction phase, of our platform. Data are represented as mean \pm SD, n = 3 independent experiments. *p < 0.05, **p < 0.01.
- (D) Intracellular flow cytometry analysis shows that nearly 100% of cells at day 2 were positive for the primitive streak TFs *T* (Brachyury), *MIXL1*, and *GSC*. Data are represented as mean \pm SD, n = 3 independent experiments.
- (E) Immunofluorescence staining shows that nearly 100% of cells at day 2 were positive for the primitive streak TFs: *T* (Brachyury), *MIXL1*, and *GSC*.
- (F) Chromatin immunoprecipitation sequencing (ChIP-seq), using H3K4me3 and H3K27me3 antibodies, shows that the *T* (Brachyury) and *WNT3* promoters were active only at day 2.



(legend on next page)



gives rise to the limb buds. qRT-PCR data showed that 40 ng/mL of exogenous BMP4, in contrast to 0–10 ng/mL BMP4 or BMP antagonism by Noggin, led to the highest levels of the lateral mesoderm markers *HAND1*, *FOXF1*, and *CD105* (endoglin), and lowest levels of the endodermal TF *GATA4* and the ectodermal TF *SOX1* (Figure 2B). Even the pluripotency TFs *OCT4*, *NANOG*, and *SOX2* resisted downregulation in the absence of BMP signaling (Figure 2C). These results were corroborated by the morphological heterogeneity observed in the absence of BMP signaling (Figure S4).

To promote cell survival and overcome the massive cell death observed during lateral mesoderm progenitor differentiation, we tested the ROCK inhibitor Y27632 and the tropomyosin-related kinase ligand neurotrophin-4, both of which had been used to promote cell survival *in vitro* (Pyle et al., 2006; Watanabe et al., 2007). Compared with neurotrophin-4, the ROCK inhibitor Y27632 increased cell numbers further by ~3-fold at day 10 (Figures 2D and 2E). More importantly, the ROCK inhibitor Y27632 dramatically increased the levels of lateral mesoderm markers (*HAND1*, *FOXF1*), relative to *GAPDH*, without increasing the expression of endodermal (*GATA4*) or ectodermal (*SOX1*) TFs (Figure 2F).

By day 10 of lateral mesoderm differentiation, the pluripotency TFs *OCT4*, *NANOG*, and *SOX2* had further decreased to 1.3%, 0.85%, and 0.77%, respectively ($p < 0.001$), relative to iPSCs (Figures 2C and S3). The primitive streak TFs *MIXL1*, *T* (Brachyury), and *GSC* were also significantly downregulated by days 8–10. The endodermal TFs (*SOX17*, *FOXA1*, *FOXA2*) and ectodermal TFs (*PAX6*, *SOX1*) also

either remained low or decreased further by day 10 (Figure S3). Paraxial mesoderm TFs *TBX6*, *MESP2*, and *MEOX2* were either downregulated or remained very low on day 10 (Figure S3), suggesting that paraxial mesoderm progenitors were not obtained. In contrast, lateral mesoderm markers, such as *HAND1* and *FOXF1* were highly upregulated by days 8–10. Interestingly, *APLNR* was also highly expressed at days 8–10 (Figure S3). *APLNR* has been previously shown to be a specific marker for mesenchymoangioblasts, a lateral mesoderm progenitor for mesenchymal and endothelial cells (Vodyanik et al., 2010). Overall by the end of lateral mesoderm progenitor differentiation, the pluripotency markers, primitive streak markers, and non-mesodermal markers were largely extinguished, while lateral mesoderm markers reached their peak.

Immunofluorescence staining for *HAND1* confirmed our qRT-PCR data, showing that nearly 100% of our cells were *HAND1*+ lateral mesoderm progenitors (Figures 2G and 2H). ChIP-seq for H3K4me3 and H3K27me3 confirmed that the *HAND1* promoter was fully activated only around day 10 (Figure 2I). Altogether these data demonstrated that hPSC-derived primitive streak cells were efficiently differentiated into lateral mesoderm progenitors, via BMP4 and ROCK inhibition, by day 10.

MSC Specification Requires Ascorbate

In phase 3 (D11–21, Figure 2A) of our platform, we aimed at the specification of skeletal MSCs, which reside in the limb skeletal bone marrow and possess the multi-lineage differentiation potential for osteogenesis, chondrogenesis, and

Figure 2. Lateral Mesoderm Differentiation Using BMP and ROCK Inhibition

(A) Schematic of three-phase protocol for differentiation of human iPSCs toward MSCs. Phase 1, the induction of primitive streak cells from human iPSCs; phase 2, differentiation into lateral mesoderm progenitors; phase 3, specification of hPSC-MSCs. The developmental stages were characterized by expression of phase-specific marker genes. A, activin A; C, CHIR99021; F, FGF; B, BMP4; R, Y27632; Fs, follistatin; P, PDGF; E, EGF; AA, ascorbic acid; PS, primitive streak.

(B) Titration of BMP4 (0–40 ng/mL) or the BMP antagonist Noggin, against lateral mesoderm differentiation, as determined by qRT-PCR for the mesoderm markers *HAND1*, *FOXF1*, and *CD105*, the endoderm TF *GATA4*, and the ectoderm TF *SOX1*, at day 10 (relative to BMP4 0 ng/mL). Data are represented as mean \pm SD, $n = 3$ independent experiments. * $p < 0.05$, ** $p < 0.01$.

(C) Titration of BMP4 or the BMP antagonist Noggin, against pluripotency markers, as determined by qRT-PCR for the pluripotency TFs *OCT4*, *NANOG*, and *SOX2*, at day 10 (relative to iPSCs). Data are represented as mean \pm SD, $n = 3$ independent experiments. * $p < 0.05$, ** $p < 0.01$.

(D) Phase contrast photomicrographs of BJ-iPSC- or MRC5-iPSC-derived primitive streak cells undergoing mesoderm differentiation, in the presence of neurotrophin-4 (NT4) or ROCK inhibitor Y27632.

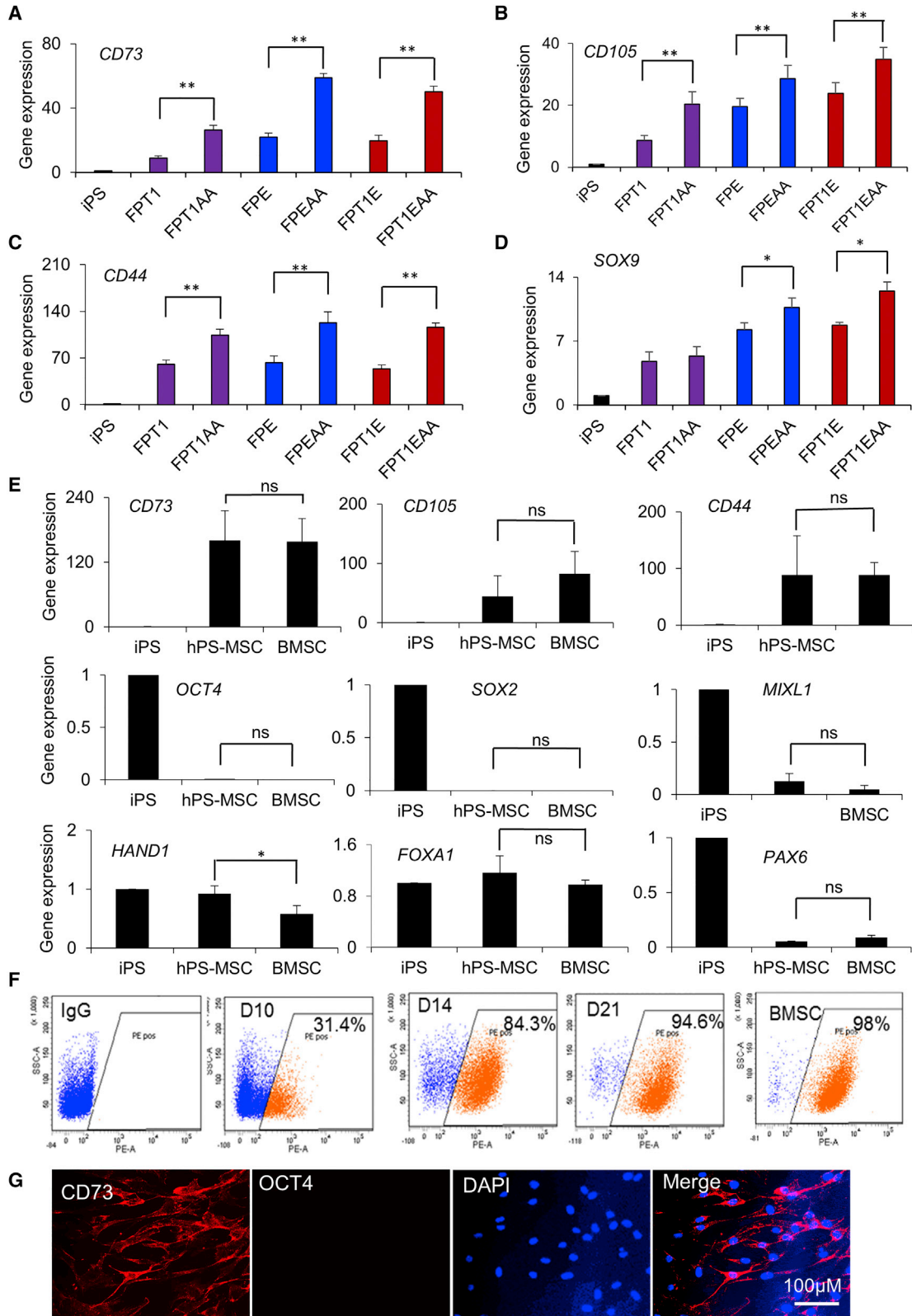
(E) Quantification of surviving live cells by trypan blue staining, during mesoderm differentiation, in the presence of neurotrophin-4 (NT4) or ROCK inhibitor Y27632 (relative to NT4). Data are represented as mean \pm SD, $n = 3$ independent experiments. * $p < 0.05$, ** $p < 0.01$.

(F) qRT-PCR for the lateral plate mesoderm markers *HAND1* and *FOXF1*, the endoderm TF *GATA4*, and the ectoderm TF *SOX1*, at day 10, in the presence of neurotrophin-4 (NT4) or ROCK inhibitor Y27632. Data are represented as mean \pm SD, $n = 3$ independent experiments. * $p < 0.05$.

(G) Immunofluorescence staining shows that nearly 100% of cells at day 10 were positive for the lateral mesoderm TF: *HAND1*.

(H) Quantitative data showed that nearly 100% of cells at d10 were positive for *HAND1* based on immunostaining against *HAND1*. Data are represented as mean \pm SD, $n = 3$ independent experiments. The percentage of *HAND1*-positive cells from different views were counted for quantification.

(I) ChIP-seq, using H3K4me3 and H3K27me3 antibodies, shows that the *HAND1* promoter was fully active only at day 10.



(legend on next page)



adipogenesis. Using different combinations and concentrations of the cytokines FGF, platelet-derived growth factor (PDGF), transforming growth factor β 1 (TGF- β 1), and epidermal growth factor (EGF), whose receptors are highly expressed in primary bone marrow MSCs (BMSCs) (Liu et al., 2007; Ng et al., 2008), we assayed for the expression of classical MSC markers. Our results showed that FGF2, PDGF, and EGF, supplemented with ascorbate, were optimal for inducing the classical MSC markers: *CD73* (ecto-5-nucleotidase), *CD105* (endoglin), *CD44* (hyaluronan receptor), and the osteochondrogenic master regulator *SOX9* (Figures 3A–3D), and classical MSC morphology (Figure S5A).

During the optimization of factors to promote specification of skeletal MSCs from lateral mesoderm progenitors, we tested the effects of ascorbate—which we had found to promote primary BMSC self-renewal earlier (Figure S5B). In nearly every combination of cytokines, ascorbate supplementation could significantly increase the expression of MSC markers, indicating that ascorbate could promote MSC specification (Figures 3A–3D). qRT-PCR results also showed that the ascorbate-induced hPSC-MSCs, which manifested primary BMSC-like levels of *CD73*, *CD105*, and *CD44* (Figure 3E), had extinguished all expression of the aforementioned pluripotency (*OCT4*, *SOX2*), mesoderm (*MIXL1*, *HAND1*), endoderm (*FOXA1*), and ectoderm (*PAX6*) TFs by day 21 (Figures 3E and S3).

FACS analysis confirmed that 94.6% of the MRC5-iPSC-derived cells were positive for the MSC marker *CD73* by day 21, similar to primary BMSCs (Figure 3F). Similar results were obtained in other hPSCs: 97.2% for BJ-iPSC-derived cells and 95.2% for H1-human embryonic stem cell (hESC)-derived cells (Figure S6), showing that this defined protocol was highly reproducible. The *CD73* qRT-PCR and FACS data were also further confirmed by immunofluorescence staining, which showed that nearly all of these cells were *CD73*+ MSCs (Figure 3G).

Characterization of hPSC-MSCs Relative to Primary BMSCs

To elucidate the molecular similarities and differences between hPSC-MSCs and primary BMSCs at the genomic level, the whole-genome transcriptome profiles of hPSC-

MSCs and BMSCs were compared with each other. The correlation coefficient between the hPSC-MSCs' transcriptome and the primary BMSCs' transcriptome was very high, $r = 0.954$ (Figure 4A). Hierarchical clustering showed that hPSC-derived cells in the intermediate phases 1–3 showed a gradual transcriptomic and epigenomic transition from the hPSC state to the hPSC-MSC state, which was remarkably similar to the primary BMSC state (Figures 4B, 4C, and S7).

Gene set enrichment analysis of the genes differentially expressed between day 10 cells (phase 2) versus hPSC-MSCs (day 21, phase 3) and BMSCs, showed that the top signature upregulated during MSC specification is the epithelial-mesenchymal transition (EMT) signature (Figure 4D). This suggests that mesoderm derivatives only fully adopt a mesenchymal identity during MSC specification. Detailed inspection of several well-known EMT markers, such as E-cadherin (*CDH1*) and *TWIST1*, confirmed this analysis (Figures 4E and 4F).

Multiplexed FACS profiling further showed that hPSC-MSCs displayed surface antigen profiles that were equivalent to primary BMSCs, being 100% negative for the blood lineage markers *CD14*, *CD34*, and *CD45*, while being nearly 100% positive for all the known BMSC surface markers *CD29*, *CD44*, *CD49c*, *CD73*, *CD90*, *CD105*, *CD151*, and *CD166* (Figure 4G).

In addition, hPSC-MSCs also expressed high levels of Gremlin mRNA and protein (Figures 4H and 4I), which had been recently shown to be a functional marker of BMSCs and skeletal stem cells (Worthley et al., 2015). Compared with primary BMSCs, hPSC-MSCs manifested similar frequencies of colony-forming unit-fibroblasts when seeded at single-cell density, suggesting that they possess a self-renewal capacity equivalent to that of primary BMSCs under the same culture conditions (Figure 4J).

We also assessed the differentiation potential of hPSC-MSCs into the three mesenchymal lineages. After 2 weeks of adipogenesis, the adipogenic markers *CEBP α* , *PPAR γ* , *LPL*, and *α 2* were highly upregulated in adipocytes derived from hPSC-MSCs (Figure 4K). Correspondingly, hPSC-MSCs were induced into osteogenesis for 2 weeks, and the osteogenic markers osteocalcin (*OC*), osteopontin (*OPN*), and *ALP* were also highly upregulated (Figure 4K).

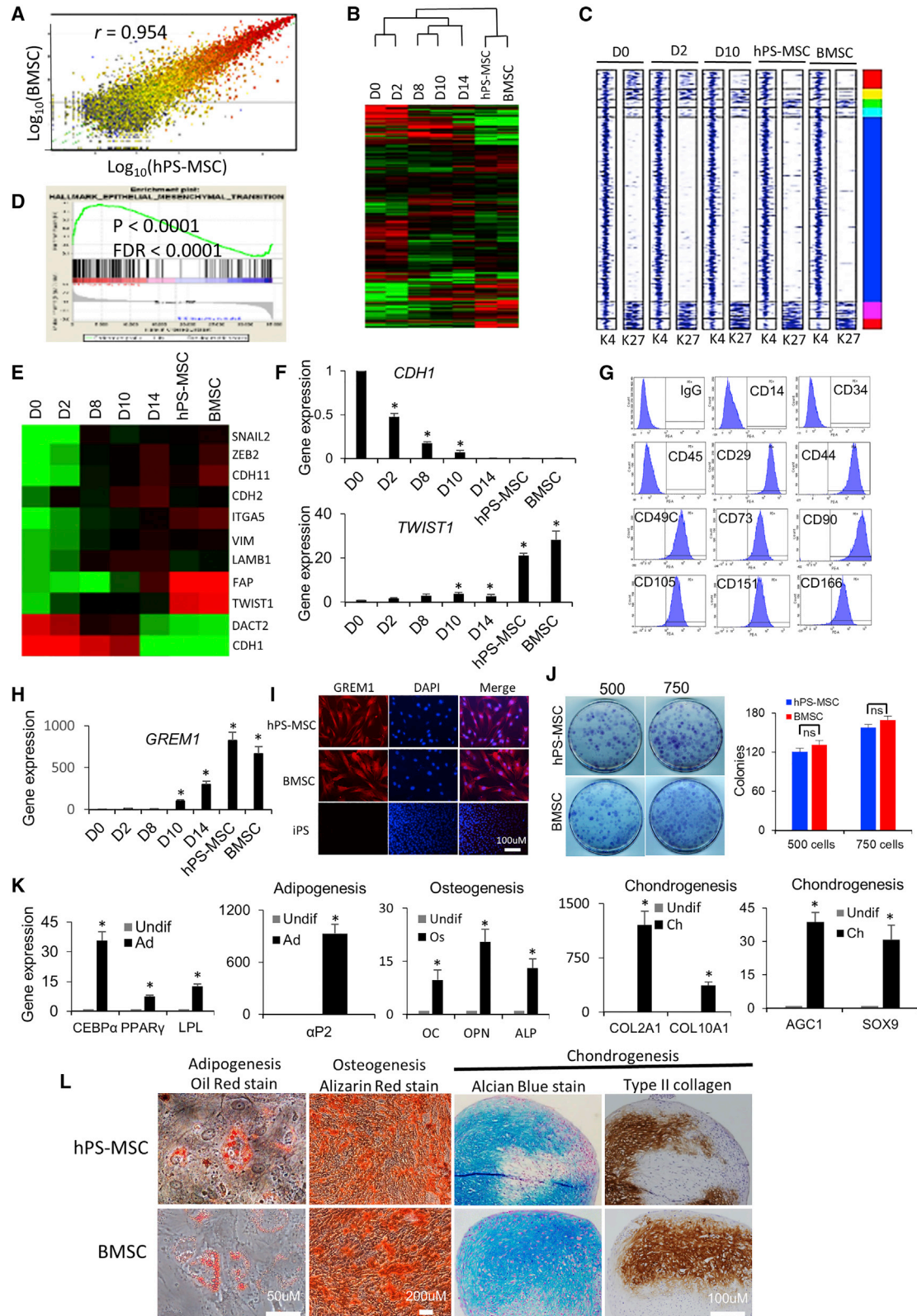
Figure 3. Ascorbate Promotes MSC Specification

(A–D) Extent of MSC specification, as determined by qRT-PCR for the classical MSC markers (A) *CD73*, (B) *CD105*, (C) *CD44*, and (D) *SOX9*, by using different combinations of FGF2 (F), PDGF (P), TGF- β 1 (T1), EGF (E), and AA. Data are represented as mean \pm SD, $n = 3$ independent experiments. * $p < 0.05$, ** $p < 0.01$.

(E) qRT-PCR for the expression levels of MSC markers (*CD73*, *CD105*, *CD44*), pluripotency markers (*OCT4*, *SOX2*), the primitive streak markers *MIXL1*, the lateral mesoderm marker *HAND1*, the endoderm marker *FOXA1*, and the ectoderm marker *PAX6*, in hPSC-MSCs and primary BMSCs, relative to iPSCs. Data are represented as mean \pm SD, $n = 3$ independent experiments. * $p < 0.05$, n.s., not significant.

(F) Flow cytometry for *CD73* expression in MRC5-iPSC-derived MSCs, relative to BMSCs.

(G) Immunofluorescence staining shows that nearly 100% of cells at day 21 were positive for *CD73*, and none were positive for *OCT4*.



(legend on next page)



The hPSC-MSCs were also induced into chondrogenesis under pellet culture conditions for 4 weeks. The chondrogenic markers *COL2A1*, *COL10A1*, *AGC1*, and *SOX9*, were also highly upregulated (Figure 4K). The hPSC-MSCs' differentiated progeny were positive for oil red staining for lipid droplets during adipogenesis, positive for alizarin red staining for bone calcium phosphate deposits during osteogenesis, and positive for Alcian blue staining for cartilaginous sulfated proteoglycans and cartilaginous type II collagen during chondrogenesis, similar to primary BMSCs (Figure 4L). Thus, the hPSC-MSCs showed robust mesenchymal tri-lineage differentiation potential, similar to primary BMSCs. To validate the complete absence of pluripotent and tumorigenic (teratoma or sarcoma) stem cells, 2×10^6 hPSC-MSCs were subcutaneously transplanted into each of six immunodeficient mice. Zero tumors were observed after 4 months in all six mice.

hPSC-MSCs Require Ascorbate and Iron

In the presence of ascorbate, we found that newly derived hPSC-MSCs showed significantly improved chondrogenic potential, compared with hPSC-MSCs derived without ascorbate, according to qRT-PCR assays for chondrogenic markers (Figure 5A). Ascorbate supplementation significantly enhanced the expression of *COL2A1* (α chain of type II collagen) and *AGC1* (aggrecan, cartilage-specific proteoglycan core protein) mRNA, while repressing the expression of *COL10A1* (α chain of type X collagen) mRNA, suggesting that ascorbate promotes hyaline cartilage rather than hypertrophic cartilage formation. This is important because hyaline cartilage is highly desirable for repairing joint articular cartilage in degenerative diseases,

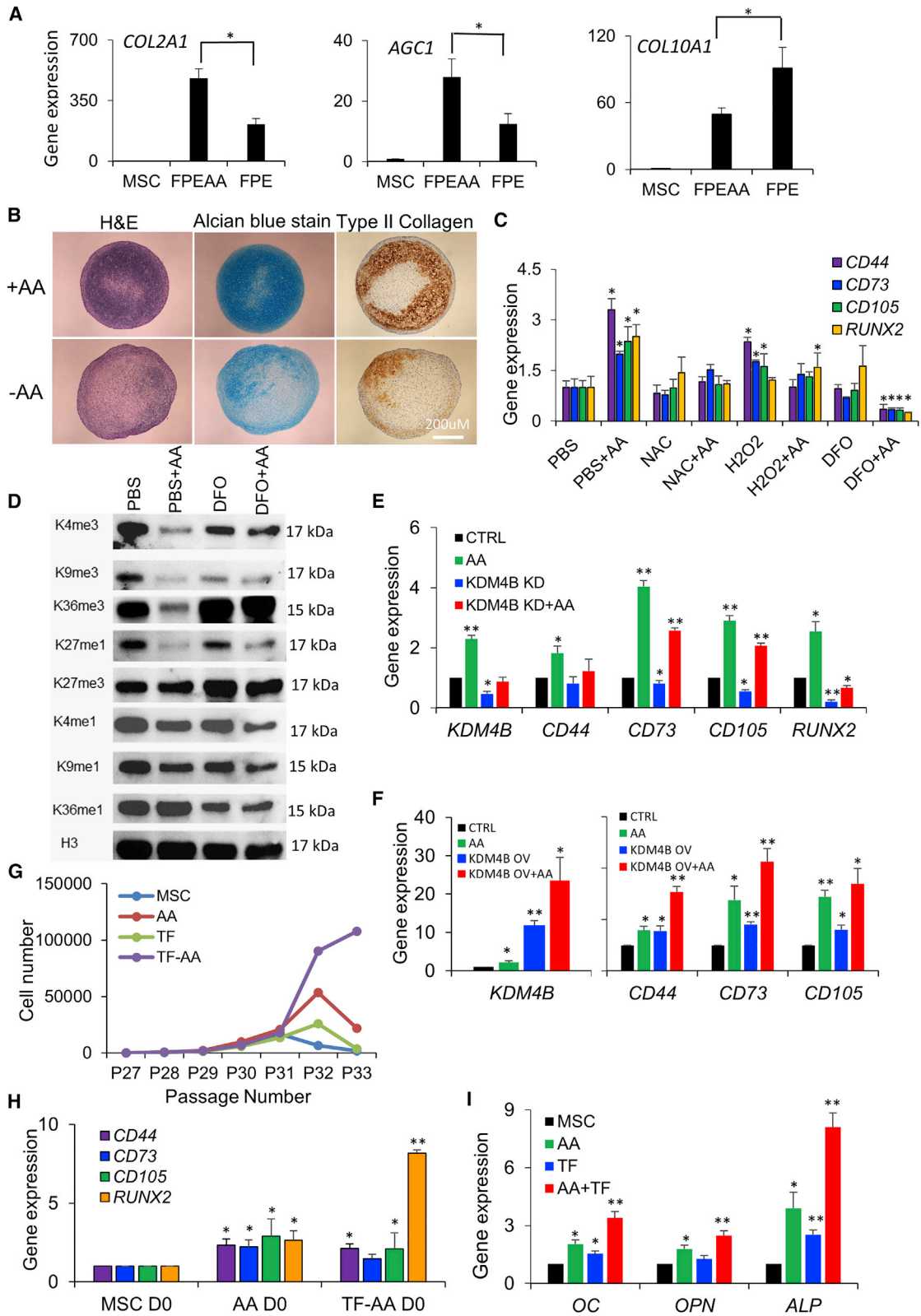
such as osteoarthritis. These mRNA results on hyaline cartilage were validated at the protein level by immunostaining for type II collagen and Alcian blue staining for sulfated proteoglycans under pellet culture conditions (Figure 5B). Ascorbate supplementation did not affect the expression of osteogenic genes (*OC* and *COL1A1*) in newly derived hPSC-MSCs that underwent osteogenesis. However, ascorbate supplementation decreased the expression of adipogenic genes (*CEBP α* and *PPAR γ*) by about 2-fold in newly derived hPSC-MSCs that underwent adipogenesis (Figure S8). Thus, our results showed that ascorbate specifically increased the chondrogenic potential of newly derived hPSC-MSCs after the specification of hPSC-MSCs.

Mechanistically, while ascorbate could serve as a cofactor to promote collagen protein synthesis (Murad et al., 1981), it could not explain the increase in collagen mRNA, and specifically the increase in *COL2A1* mRNA and the decrease in *COL10A1* mRNA. It also could not explain ascorbate's induction of the MSC markers, *CD73*, *CD105*, and *CD44*, and the osteochondrogenic TF *SOX9* (Figures 3A–3D).

Ascorbate metabolism is known to exert pleiotropic effects on cells. In fact, ascorbate could also serve as an antioxidant to scavenge reactive oxygen species (ROS), or help MSCs regenerate another cellular antioxidant, glutathione. Thus, to examine if redox regulation was the mechanistic basis of ascorbate's effects on MSC specification, we applied the antioxidant N-acetyl-cysteine (NAC) and the ROS-producing hydrogen peroxide (H_2O_2) during the specification of hPSC-MSCs. Although we expected NAC to mimic ascorbate, and H_2O_2 to block ascorbate's effects, we found the opposite to be true (Figure 5C). NAC robustly blocked the positive effects of ascorbate on MSC markers, whereas

Figure 4. Characterization of hPSC-MSCs, Relative to Primary BMSCs

- (A) Correlation plot for \log_{10} -transformed expression values of all genes in the hPSC-MSC transcriptome versus BMSC transcriptome.
- (B) Hierarchical clustering of the transcriptomic profiles for each phase (D0–21) of hPSC-MSC derivation versus primary BMSCs.
- (C) Hierarchical clustering of the H3K4me3 and H3K27me3 ChIP-seq density plots for each phase of hPSC-MSC derivation versus primary BMSCs. Genomic loci with similar temporal patterns were classified by color.
- (D) Gene set enrichment analysis of the differentially expressed genes for lateral mesoderm progenitors at D10 versus both hPSC-MSCs and primary BMSCs, revealed that the top hallmark signature is an upregulation of the epithelial-mesenchymal transition (EMT) signature in MSCs.
- (E) Heatmap depicting the expression levels of EMT genes during hPSC-MSC derivation.
- (F) qRT-PCR for *CDH1* and *TWIST1* during hPSC-MSC derivation. Data are represented as mean \pm SD, $n = 3$ independent experiments. * $p < 0.05$.
- (G) Surface antigen profiling of hPSC-MSCs using the known surface markers for BMSCs.
- (H) qRT-PCR for *GREM1* during hPSC-MSC derivation. Data are represented as mean \pm SD, $n = 3$ independent experiments. * $p < 0.05$.
- (I) Immunofluorescence staining shows that nearly 100% of hPSC-MSCs and BMSCs were positive for *GREM1*.
- (J) Colony-forming unit-fibroblast (CFU-F) assay for hPSC-MSCs, relative to primary BMSCs.
- (K) qRT-PCR for adipogenic markers (Ad: *CEBP α* , *PPAR γ* , *LPL*, *$\alpha P2$*), osteogenic markers (Os: *OC*, *OPN*, *ALP*), and chondrogenic markers (Ch: *COL2A1*, *COL10A1*, *AGC1*, *SOX9*), relative to undifferentiated hPSC-MSCs (Undif), during the tri-lineage differentiation assay. Data are represented as mean \pm SD, $n = 3$ independent experiments. * $p < 0.05$.
- (L) Oil red staining for lipid droplets after adipogenesis, alizarin red staining for calcium deposits after osteogenesis, Alcian blue staining for sulfated proteoglycans, and type II collagen immunostaining after chondrogenesis, during the tri-lineage differentiation assay for hPSC-MSCs, relative to BMSCs.



(legend on next page)



H₂O₂ increased the MSC markers *CD44*, *CD73*, and *CD105*. Instead, these results suggested that some levels of ROS were in fact necessary for the specification of MSCs from lateral mesoderm progenitors, and that the antioxidant function of ascorbate could not have been the mechanistic reason for its promotion of MSC specification.

Another metabolic function of ascorbate is to serve as a cofactor for a family of enzymes known as the ascorbate/iron-dependent dioxygenases. If ascorbate was indeed promoting MSC specification via the ascorbate/iron-dependent dioxygenases, then it would imply that iron sequestration would block ascorbate's positive effects on MSC markers. We found that some iron sequestration by low concentrations of desferrioxamine (DFO) did robustly abrogate the positive effects of ascorbate, without any toxicity to hPSC-MSCs on its own, indicating that DFO blocked MSC specification in an ascorbate-dependent manner (Figure 5C). Conversely, these data also implied that ascorbate promoted MSC specification in an iron-dependent manner.

One important subgroup of the ascorbate/iron-dependent dioxygenases is the JmjC histone demethylases that regulate the chromatin epigenetic state. To assess the effects of ascorbate on histone methylation during MSC specification, we performed a series of western blots for different histone H3 lysine residues' methylation status. We observed that ascorbate robustly reduced H3K4me3, H3K9me3, H3K36me3, and H3K27me1, relative to the PBS control (Figure 5D). Most other H3 lysine methylation marks remained unchanged. These results suggest that ascorbate promoted MSC specification via a subgroup of JmjC histone demethylases. To test if ascorbate was acting on these H3 methyl-lysines via iron-dependent demethy-

lases, we first added DFO to the cells during MSC specification, with and without ascorbate. Our results showed that only the specific H3 methyl-lysine marks reduced by ascorbate, were specifically increased by DFO (Figure 5D), indicating that the ascorbate-mediated H3 lysine demethylation was indeed iron-dependent.

To further test if ascorbate promoted the specification of hPSC-MSCs via JmjC ascorbate/iron-dependent histone demethylases, we knocked down and overexpressed the H3K9me3 demethylase *KDM4B*. *KDM4B*, also known as *JMJD2B*, is a JmjC domain-containing histone demethylase that is specifically involved in the demethylation of repressive H3K9 tri-methylation, which is one of the four H3 Lys residues affected by our ascorbate treatment of hPSC-MSCs. Our data showed that ascorbate supplementation alone increased the expression of *KDM4B* (Figures 5E and 5F), as well as other MSC markers. *KDM4B* knockdown with lentiviral short hairpin RNA (shRNA) decreased the expression of the MSC markers *CD44*, *CD73*, *CD105*, and *RUNX2*, both in the absence and presence of ascorbate, although ascorbate supplementation did partially rescue several MSC markers after *KDM4B*'s partial knockdown (Figure 5E). *KDM4B* lentiviral overexpression further increased the expression of MSC genes, both in the absence and presence of ascorbate (Figure 5F). These results suggest that *KDM4B* is both necessary and sufficient for hPSC-MSC specification, and that *KDM4B* lies downstream of ascorbate.

Conversely, when we supplemented the ascorbate-containing media with iron, by adding transferrin, we observed a large increase in the self-renewal capacity of hPSC-MSCs, which would otherwise undergo senescence and apoptosis over long-term culture (Figure 5G). Ascorbate-treated hPSC-MSCs still retained the capacity for colony formation

Figure 5. hPSC-MSCs Require Ascorbate and Iron for the Specification and Long-Term Self-Renewal

- (A) qRT-PCR for the chondrogenic markers *COL2A1*, *AGC1*, and *COL10A1*, after chondrogenic differentiation of hPSC-MSCs induced in FPE or FPEAA (FGF2, PDGF, EGF, ascorbate), relative to undifferentiated MSCs. Data are represented as mean \pm SD, n = 3 independent experiments. *p < 0.05.
- (B) Type II collagen immunostaining and Alcian blue staining of chondrogenic pellets derived from hPSC-MSCs induced in FPE or FPEAA (FGF2, PDGF, EGF, AA).
- (C) qRT-PCR for the classical MSC markers, *CD44*, *CD73*, *CD105*, and *RUNX2*, in hPSC-MSCs cultured in the presence of AA, and/or the antioxidant NAC, and/or hydrogen peroxide (H₂O₂), and/or the iron chelator desferrioxamine (DFO), relative to PBS control. Data are represented as mean \pm SD, n = 3 independent experiments. *p < 0.05.
- (D) Western blots for histone H3 lysine methylation in hPSC-MSCs cultured in the presence of AA, and/or the iron chelator DFO, relative to PBS control.
- (E) qRT-PCR for the classical MSC markers in hPSC-MSCs with or without lentiviral shRNA knockdown (KD) of *KDM4B*, cultured with or without AA supplementation. Data are represented as mean \pm SD, n = 3 independent experiments. *p < 0.05, **p < 0.01.
- (F) qRT-PCR for the classical MSC markers in hPSC-MSCs with or without lentiviral overexpression (OV) of *KDM4B*, cultured with or without AA supplementation. Data are represented as mean \pm SD, n = 3 independent experiments. *p < 0.05, **p < 0.01.
- (G) Proliferation curve for hPSC-MSCs cultured in the presence of AA, or transferrin (TF), or both (TF + AA), relative to PBS control.
- (H) qRT-PCR for the classical MSC markers, *CD44*, *CD73*, *CD105*, *RUNX2*, in hPSC-MSCs cultured in the presence of AA, or TF and AA (TF + AA). Data are represented as mean \pm SD, n = 3 independent experiments. *p < 0.05, **p < 0.01.
- (I) qPCR for osteogenic markers of hPSC-MSCs supplemented with AA, TF, or both (TF + AA) and subjected to osteogenic differentiation. Data are represented as mean \pm SD, n = 3 independent experiments. *p < 0.05, **p < 0.01.



and tri-lineage differentiation after long-term culture (Figure S9). Although either ascorbate or transferrin alone could promote hPSC-MSC proliferative potential, neither could increase hPSC-MSC proliferative potential as much as the combination of both ascorbate and transferrin (Figure 5G). Moreover, ascorbate/transferrin-treated hPSC-MSCs were also significantly higher in their expression of MSC markers than the vehicle control, especially the osteogenic TF *RUNX2* (Figure 5H), suggesting improved osteochondrogenic differentiation potential after ascorbate/transferrin treatment. Indeed, we found that transferrin synergized with ascorbate to enhance the long-term osteogenic potential of hPSC-MSCs (Figure 5I). Together with our chondrogenesis results (Figure 5B), our data support the idea that hPSC-MSCs require ascorbate and iron to maintain long-term self-renewal of MSC identity and long-term osteochondrogenic differentiation potential, both of which diminish with aging in MSCs.

Repair of Cartilage Defects by hPSC-MSCs

To assess the functionality of hPSC-MSCs *in vivo*, we sought to test their potency in repairing joint articular cartilage defects *in vivo*—potentially one of the most important applications of hPSC-MSCs. Primary BMSCs were considered as the gold standard to assess hPSC-MSCs. We orthotopically transplanted both hPSC-MSCs and primary BMSCs, which were subjected to chondrogenesis *in vitro* for 7 days under pellet conditions, into cartilage defects created in the joint articular surface of immunosuppressed rats (Liu et al., 2011). Six weeks after orthotopic transplantation, the defects were filled with engrafted tissue derived from the transplanted pellets. The engrafted tissue was positive for Alcian blue staining for sulfated proteoglycans and immunostaining for type II collagen, compared with the sham control (Figure 6A), showing that new cartilage similar to the adjacent host cartilage was being formed. Histological grading score showed that both hPSC-MSCs and primary BMSCs significantly improved cartilage repair compared with the sham control. There was no significant difference in the histological grading scores between hPSC-MSCs and primary BMSCs (Figure 6B). Immunostaining against the human-specific antigen lamin A/C showed that the engrafted cells were well-integrated into the adjacent host cartilage (Figure 6C). At week 6, however, the apical edges of the hPSC-MSC- and BMSC-derived grafts were still negative for Alcian blue staining and type II collagen immunostaining (Figure 6A) suggested that the repair of cartilage defects was still not complete.

At week 12, the hPSC-MSC-derived graft was well-integrated with all edges of the adjacent host cartilage. Most importantly, the hPSC-MSC-derived graft showed intensely positive Alcian blue staining for sulfated proteoglycans and type II collagen immunostaining, even at the

apical surface (Figure 6D). At 12 weeks, the histological grading scores for both hPSC-MSC-derived cartilage and BMSC-derived cartilage improved even further from 6 weeks, and in fact the hPSC-MSC-derived cartilage appeared slightly better than primary BMSC-derived cartilage (Figures 6D and 6E). Immunostaining against the human-specific antigen lamin A/C confirmed that the engrafted human cells continued to be well-integrated into the adjacent host cartilage at 12 weeks (Figure 6F).

Taken together, our hPSC-MSCs fully resemble primary BMSCs epigenetically, transcriptionally and functionally, both *in vitro* and *in vivo*, as shown by their ability to repair joint articular cartilage defects. These data also suggest that ascorbate/transferrin-treated hPSC-MSCs could provide an alternative, patient-specific source of autologous cells for cartilage repair and regeneration in future.

DISCUSSION

By modeling the different phases of embryonic development that lead from hPSCs to skeletal MSCs, we have generated a platform to dissect human MSC specification. Our platform for generating skeletal MSCs from hPSCs represents a stepwise recapitulation of lateral mesoderm and appendicular skeleton development to derive MSCs with high efficiency. It is a chemically defined platform, freed of feeders to minimize the biological variability of the resultant MSCs, and a metabolically optimized platform to enhance MSCs' long-term self-renewal and osteochondrogenic capacities.

In the process, we discovered that ROCK inhibition promotes lateral mesoderm progenitor proliferation, and that ascorbate promotes MSC specification. Moreover, we found that ascorbate promotes MSCs' long-term self-renewal and osteochondrogenic potential in an iron-dependent fashion. This mechanism operated, in part, through ascorbate/iron-dependent dioxygenases, including a subgroup of JmjC histone demethylases.

Our histone methylation results suggested that at least four families of JmjC dioxygenases could be involved: the JMJD2 family of H3K9me3 demethylases, the JARID1 family of H3K4me3 demethylases, the JMJD3 family of H3K27me1 demethylases, and the JMJD2 family of H3K36me3 demethylases (Cloos et al., 2008). Our results further showed that KDM4B (JMJD2B) was necessary and sufficient to promote ascorbate-driven MSC specification, suggesting that ascorbate promoted the specification of hPSC-MSCs at least in part via the H3K9me3 demethylase KDM4B.

Given the importance of ascorbate/iron-dependent dioxygenases in cell fate decisions, the broad implications of optimizing the ascorbate/transferrin concentrations could

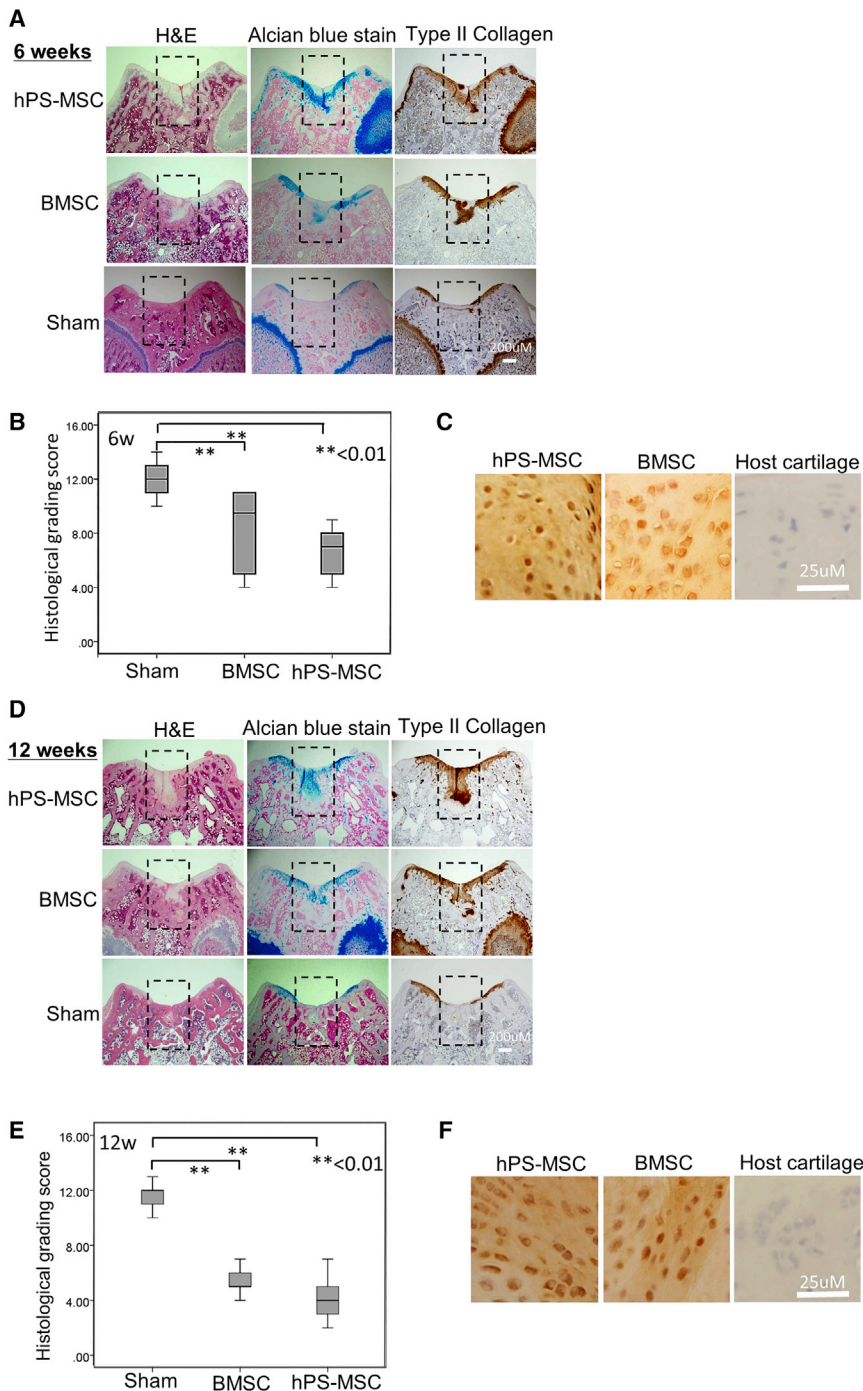


Figure 6. hPSC-MSCs Can Fully Repair and Regenerate Articular Joint Cartilage

(A) After 6 weeks, H&E staining, type II collagen immunostaining, and Alcian blue staining of rat knee joint cartilage defects (dotted box) transplanted with hPSC-MSC- and primary BMSC-derived chondrogenic pellets, relative to the sham control.

(B) Histological grading scores for rat knee joint cartilage defects after 6 weeks of transplantation with hPSC-MSC- and primary BMSC-derived chondrogenic pellets, relative to the sham control (** $p < 0.01$).

(C) Immunostaining for human-specific lamin A/C showed positive human chondrocytes integrated into the rat knee joint cartilage after transplantation with hPSC-MSCs and primary BMSCs, but not in the sham control after 6 weeks of transplantation.

(D) After 12 weeks, H&E staining, type II collagen immunostaining, and Alcian blue staining of rat knee joint cartilage defects (dotted box) transplanted with hPSC-MSC- and primary BMSC-derived chondrogenic pellets, relative to the sham control.

(E) Histological grading scores for rat knee joint cartilage defects after 12 weeks of transplantation with hPSC-MSC- and primary BMSC-derived chondrogenic pellets, relative to the sham control (** $p < 0.01$).

(F) Immunostaining for human-specific lamin A/C showed positive human chondrocytes integrated into the rat knee joint cartilage after transplantation with hPSC-MSCs and primary BMSCs, but not in the sham control after 12 weeks of transplantation.

go beyond MSC specification *in vitro*. Already, it is well known that ascorbate is very useful in promoting iPSC reprogramming (Chen et al., 2013; Chung et al., 2010; Wang et al., 2011). It is possible that tailoring the ascorbate/transferrin concentrations for particular cell types, beyond MSCs, could be useful for enhancing the specification and self-renewal of other adult stem cells *in vitro*. These

findings also have important implications for our understanding of how nutritional supplementation with optimal ascorbate/iron concentrations could affect the self-renewal and maintenance of different stem cell populations in our body during aging *in vivo*. For example, it is thought that defects in adult MSC self-renewal, in part due to increasing H3K9me3 in aging bone, is responsible for osteoporosis



during aging (Ye et al., 2012). Our results suggest that supplementing the correct ascorbate/iron concentrations for JmjC demethylases in MSCs in the human body might ameliorate the effects of aging on bone and cartilage diseases in future. Because the enzyme for ascorbate synthesis, L-gulonolactone oxidase, was only recently lost in primate evolution, it is possible that optimal ascorbate supplementation could be especially pertinent for somatic stem cells and their aging in human physiology.

EXPERIMENTAL PROCEDURES

Generation of iPSCs

Human iPSCs were generated by infecting fibroblasts of MRC5 or BJ cells with OCT4, SOX2, KLF4, or c-MYC retroviruses, as reported previously (Takahashi et al., 2007). GP2 cell were transfected with the four plasmids and the retrovirus was harvested 48 h after transduction. Fibroblasts were infected with harvested retrovirus. Five days after infection, infected MRC5 or BJ cells were plated onto mouse embryonic fibroblast feeder cells treated with mitomycin C and cultured in human ES medium to generate iPSCs. The generated iPSCs and the commercial hESC line H1 were used to define the differentiation protocol.

Differentiation of hPSCs into MSCs

Feeder-free human hPSCs were maintained in mTeSR (STEMCELL Technologies) before differentiation. To differentiate hPSCs into MSCs, hPSCs were digested with 1 mg/mL collagenase IV for 5–10 min at 37°C into small clumps and placed on a fibronectin-coated surface in medium containing activin A (25 ng/mL) and CHIR99021 (3 μ M) for 1 day in a basal medium (DMEM: F12, 1% ITS, 2% B27, 2 mM L-glutamine, 90 μ M β -mercaptoethanol), followed by activin A (25 ng/mL), CHIR99021 (3 μ M), and FGF2 (20 ng/mL) for a further 24 h to differentiate toward primitive streak cells. Mesoderm differentiation was then induced with FGF2 (20 ng/mL), BMP4 (40 ng/mL), ROCK inhibitor Y27632 (5 μ M), and follistatin (100 ng/mL) for 8 days. MSCs were then specified and matured with FGF2 (50 ng/mL), PDGF (50 ng/mL), EGF (100 ng/mL), and ascorbic acid (500 μ g/mL) (Table S1) for another 11 days. The hPSC-MSCs were passaged 1:3 with accutase and maintained under subconfluent conditions for each passage.

Directed differentiation toward MSCs was assessed by qRT-PCR for expression of genes associated with pluripotency, primitive streak, mesoderm, endoderm, ectoderm, and MSCs (Table S2), and immunostaining or FACS (Table S3).

Primary MSCs Derived from Human Bone Marrow

Human BMSCs were cultured from bone marrow aspirated from patients, as described previously (Liu et al., 2007), and in accordance with ethical legislation and the National University Hospital institutional review board guidelines. In brief, 2- to 10-mL bone marrow aspirates were taken after informed consent. Nucleated cells were isolated with a density gradient (Ficoll-Pharmacia) and resuspended in complete culture medium. All of the nucleated cells were plated in 25 mL medium in a culture dish and incubated at 37°C with 5% CO₂. After 24 h, nonadherent cells were discarded,

and adherent cells were thoroughly washed twice with PBS. The cells were incubated for 5–7 days, harvested with 0.25% trypsin and 1 mM EDTA for 5 min at 37°C, replated at 6 cells/cm² in culture flasks. To prevent spontaneous differentiation, cells were maintained at subconfluent levels.

Flow Cytometry

The hPSC-MSCs were harvested in 0.25% trypsin/EDTA, washed with FACS buffer (PBS + 0.5% BSA + 5 mM EDTA), and then incubated for 30 min in dark in FACS buffer containing phycoerythrin (PE)-conjugated antibodies against the following surface antigens: CD14, CD34, CD45, CD29, CD44, CD49C, CD73, CD90, CD105, CD151, and CD166. Cells were washed and resuspended in FACS buffer for analysis. Cells were stained with PE-conjugated nonspecific immunoglobulin G to assess background fluorescence (Table S3).

Osteogenic, Chondrogenic, and Adipogenic Differentiation Assays

hPSC-MSCs were cultured under subconfluent conditions to prevent spontaneous differentiation. MSCs were induced to differentiate toward adipocytes in adipogenic medium and osteoblasts in osteogenic medium for 14 days, as described previously (Liu et al., 2007). A pellet culture system, as described previously (Liu et al., 2007), was used for chondrocyte differentiation for 28 days. Cells in growth medium were used as control. Adipogenic medium contained 0.5 mM isobutyl-methylxanthine, 1 μ M dexamethasone, 10 μ M insulin, 200 μ M indomethacin, and 1% antibiotic/antimycotic. Osteogenic medium contained 0.1 μ M dexamethasone, 50 μ M ascorbate-2-phosphate, 10 mM β -glycerophosphate, and 1% antibiotic/antimycotic. Chondrogenic medium contained 10 ng/mL TGF- β 3, 0.1 μ M dexamethasone, 50 μ g/mL ascorbate-2-phosphate, 40 μ g/mL proline, 100 μ g/mL pyruvate, and 50 mg/mL ITS+ Premix (Becton Dickinson; 6.25 μ g/mL insulin, 6.25 μ g/mL transferrin, 6.25 μ g/mL selenious acid, 1.25 mg/mL BSA, and 5.35 mg/mL linoleic acid). The supplements were purchased from Sigma, unless otherwise stated. The medium was replaced every 3–4 days. Differentiation of MSCs was evaluated by qRT-PCR and lineage-specific staining: oil red O staining for lipid droplets in adipogenesis, alizarin red S staining for calcium deposits in osteogenesis, type II collagen immunostaining for the major collagen of cartilage, and Alcian blue staining for cartilage proteoglycans in chondrogenesis.

Quantitative Real-Time PCR

Quantitative real-time PCR was performed using an ABI PRISM 7900HT sequence Detection System (Applied Biosystems). In brief, 0.5 μ g of total RNA was converted to cDNA using a high-capacity cDNA archive kit in 30 μ L and then diluted to 500 μ L. Diluted cDNA was used for qRT-PCR in a 384-well high-throughput format. For each individual qRT-PCR reaction per well of 10 μ L, 5 μ L of 2X SYBR Green Master Mix (Applied Biosystems) was used and combined with 0.5 μ L of a combined forward and reverse primer mix (at 10 μ M of forward + reverse primers in the combined primer mix). The expression of experimental genes was internally normalized to the expression of a human housekeeping gene (*GAPDH*) for that same cDNA sample.



Microarray Analysis

Total RNA was isolated using an RNeasy Mini Kit (QIAGEN, Chatsworth, CA) per the manufacturer's protocol. In brief, 0.3 µg total RNA was used to synthesize cRNA (Illumina TotalPrep RNA Amplification Kit, Ambion). The cRNA was then hybridized to Illumina Human HT-12 microarrays according to the manufacturers' instructions. The data were analyzed using software GeneSpring v.12.5. All microarray data are available from the GEO (<http://www.ncbi.nlm.nih.gov/geo>) under accession code GSE140450.

ChIP-Seq

For ChIP-seq, samples were fixed with formaldehyde, lysed, sonicated, and precleared. The chromatin was probed overnight using H3K4me3 and H3K27me3 antibodies (Abcam) conjugated to Protein G Dynabeads (Invitrogen). Subsequently, chromatin was precipitated, rigorously washed, and de-crosslinked overnight at 65°C. Ten nanograms of chromatin were used to generate libraries (TruSeq Kit, Illumina) for HiSeq 2000 Sequencing (Illumina, 72 bp single-end reads). Reads were aligned to hg19.

Tumorigenicity Assay

To validate the loss of pluripotency in hPSC-MSCs, hPSC-MSCs were harvested by trypsinization and washed twice with PBS, viable cell number was determined by trypan blue exclusion. hPSC-MSCs (2×10^6) suspended in Matrigel were subcutaneously transplanted into the flanks of 6-week-old immunodeficient nude mice. This assay was performed on six mice. The mice were kept in pathogen-free conditions and observed for 4 months to monitor tumor formation. All experiments involving animals were conducted under approved protocols granted by the A*STAR Institutional Animal Care and Use Committee.

Loss or Gain of Function of *KDM4B*

KDM4B was knocked down or overexpressed by lentiviral shRNA or cDNA, respectively, for stable expression. Lentiviral plasmids of *KDM4B* (Origene) were cotransfected with packaging vectors into 293FT cells. Supernatants were harvested after 48 h. Human lateral mesoderm progenitor cells at phase 2 of the differentiation protocol were infected with the lentiviral supernatants, containing 8 µg/mL Polybrene, to achieve stable knockdown or overexpression. The effects of knockdown or overexpression on the specification of hPSC-MSCs were examined at day 21 of differentiation.

Transplantation of hPSC-MSCs into Rats for Cartilage Repair Assay

hPSC-MSCs were transplanted into cartilage defects of rats as described previously (Liu et al., 2011). BMSCs were used as the gold standard control to assess hPSC-MSCs. BMSCs were used as positive controls in this study. In brief, male Sprague-Dawley rats (500 g) were anesthetized using an intraperitoneal injection of a mixture of ketamine (10 mg/100 g) and xylazine (1 mg/100 g). An anterior midline incision was made through the skin of the knee. The knee joints were opened via a medial parapatellar approach and the patella was everted. An osteochondral defect

(1.5 mm in diameter and 1.5 mm in depth) was created in the patellar groove of the distal femur. Pellets from hPSC-MSCs or BMSCs were transplanted into cartilage defects, with the defects without transplanted cells serving as the control. The pellets from 3×10^5 hPSC-MSCs or BMSCs were preinduced into chondrocyte differentiation for 1 week before transplantation as described previously (Liu et al., 2011). The recipient animals received daily subcutaneous injections of cyclosporine (14 mg/kg, Novartis Pharma AG, Basel, Switzerland) immediately after surgery.

At 6 and 12 weeks after surgery, rats from each group were sacrificed. The distal femurs with the cartilage defects were harvested and fixed in 10% buffered formalin. The tissues were decalcified and cut into 5-µm sections. Staining was performed with H&E, type II collagen immunostaining, and Alcian blue staining for sulfated proteoglycans in the cartilage matrix. Each sample was graded by an independent histopathologist according to the histological scale as described previously (Wakitani et al., 1994). The scale consists of five categories: cell morphology, matrix staining, surface regularity, thickness of cartilage, and integration of donor with host cartilage. The scores range from 0 (normal articular cartilage) to 14 (no cartilaginous tissue), at least 10 defects from each group were assessed.

Statistical Analysis

Comparisons of histological scores for cartilage repair were performed using the Mann-Whitney U test for nonparametric analyses. Otherwise, statistical analyses were performed using Student's unpaired two-tailed t tests. p values less than 0.05 were considered statistically significant.

SUPPLEMENTAL INFORMATION

Supplemental Information can be found online at <https://doi.org/10.1016/j.stemcr.2020.01.002>.

AUTHOR CONTRIBUTIONS

T.M.L., B.L., and N.S.-C. designed the study. T.M.L., P.L., H.T.F., E.D.Y., and D.V. performed the experiments. T.M.L., V.K., Y.H.L., E.H.L., B.L., N.S.-C., S.M.C., B.T.T., and J.H.H., analyzed the data. N.S.-C., T.M.L., and B.L. wrote the paper.

ACKNOWLEDGMENTS

The defined protocol has been filed for US and Singapore patent. The authors have no additional conflict of interest. This work was supported by the National Key R&D Program of China (2019YFA0801701), the Strategic Priority Research Program of the CAS (XDA16020301), the Key Research Program of the CAS (KJZD-SW-L04), the NMRC OF-IRG (NMRC/OFIG/0031/2016), and A*STAR. The sponsors had no role in the study design, data collection, data analysis, data interpretation, or writing of the article. We thank all our lab members and institutional colleagues for helpful suggestions and feedback on our study.

Received: February 1, 2019
Revised: December 31, 2019
Accepted: January 2, 2020
Published: January 30, 2020



REFERENCES

- Alman, B.A. (2015). The role of hedgehog signalling in skeletal health and disease. *Nat. Rev. Rheumatol.* *11*, 552–560.
- Barberi, T., Willis, L.M., Socci, N.D., and Studer, L. (2005). Derivation of multipotent mesenchymal precursors from human embryonic stem cells. *PLoS Med.* *2*, e161.
- Chen, J., Guo, L., Zhang, L., Wu, H., Yang, J., Liu, H., Wang, X., Hu, X., Gu, T., Zhou, Z., et al. (2013). Vitamin C modulates TET1 function during somatic cell reprogramming. *Nat. Genet.* *45*, 1504–1509.
- Chung, T.L., Brena, R.M., Kolle, G., Grimmond, S.M., Berman, B.P., Laird, P.W., Pera, M.F., and Wolvetang, E.J. (2010). Vitamin C promotes widespread yet specific DNA demethylation of the epigenome in human embryonic stem cells. *Stem Cells* *28*, 1848–1855.
- Cloos, P.A., Christensen, J., Agger, K., and Helin, K. (2008). Erasing the methyl mark: histone demethylases at the center of cellular differentiation and disease. *Genes Dev.* *22*, 1115–1140.
- Gadue, P., Huber, T.L., Paddison, P.J., and Keller, G.M. (2006). Wnt and TGF-beta signaling are required for the induction of an in vitro model of primitive streak formation using embryonic stem cells. *Proc. Natl. Acad. Sci. U S A* *103*, 16806–16811.
- Hwang, N.S., Varghese, S., Lee, H.J., Zhang, Z., Ye, Z., Bae, J., Cheng, L., and Elisseeff, J. (2008). In vivo commitment and functional tissue regeneration using human embryonic stem cell-derived mesenchymal cells. *Proc. Natl. Acad. Sci. U S A* *105*, 20641–20646.
- Li, Y., Zhang, W., Chang, L., Han, Y., Sun, L., Gong, X., Tang, H., Liu, Z., Deng, H., Ye, Y., et al. (2016). Vitamin C alleviates aging defects in a stem cell model for Werner syndrome. *Protein Cell* *7*, 478–488.
- Liu, P., Wakamiya, M., Shea, M.J., Albrecht, U., Behringer, R.R., and Bradley, A. (1999). Requirement for Wnt3 in vertebrate axis formation. *Nat. Genet.* *22*, 361–365.
- Liu, T.M., Martina, M., Hutmacher, D.W., Hui, J.H., Lee, E.H., and Lim, B. (2007). Identification of common pathways mediating differentiation of bone marrow and adipose tissues derived human mesenchymal stem cells (MSCs) into three mesenchymal lineages. *Stem Cells* *25*, 250–260.
- Liu, T.M., Guo, X.M., Tan, H.S., Hui, J.H., Lim, B., and Lee, E.H. (2011). Zinc-finger protein 145, acting as an upstream regulator of SOX9, improves the differentiation potential of human mesenchymal stem cells for cartilage regeneration and repair. *Arthritis Rheum.* *63*, 2711–2720.
- Murad, S., Grove, D., Lindberg, K.A., Reynolds, G., Sivarajah, A., and Pinnell, S.R. (1981). Regulation of collagen synthesis by ascorbic acid. *Proc. Natl. Acad. Sci. U S A* *78*, 2879–2882.
- Ng, F., Boucher, S., Koh, S., Sastry, K.S., Chase, L., Lakshmipathy, U., Choong, C., Yang, Z., Vemuri, M.C., Rao, M.S., et al. (2008). PDGF, TGF-beta, and FGF signaling is important for differentiation and growth of mesenchymal stem cells (MSCs): transcriptional profiling can identify markers and signaling pathways important in differentiation of MSCs into adipogenic, chondrogenic, and osteogenic lineages. *Blood* *112*, 295–307.
- Nostro, M.C., Cheng, X., Keller, G.M., and Gadue, P. (2008). Wnt, activin, and BMP signaling regulate distinct stages in the developmental pathway from embryonic stem cells to blood. *Cell Stem Cell* *2*, 60–71.
- Olivier, E.N., Rybicki, A.C., and Bouhassira, E.E. (2006). Differentiation of human embryonic stem cells into bipotent mesenchymal stem cells. *Stem Cells* *24*, 1914–1922.
- Prockop, D.J. (2009). Repair of tissues by adult stem/progenitor cells (MSCs): controversies, myths, and changing paradigms. *Mol. Ther.* *17*, 939–946.
- Pyle, A.D., Lock, L.F., and Donovan, P.J. (2006). Neurotrophins mediate human embryonic stem cell survival. *Nat. Biotechnol.* *24*, 344–350.
- Takahashi, K., Tanabe, K., Ohnuki, M., Narita, M., Ichisaka, T., Tomoda, K., and Yamanaka, S. (2007). Induction of pluripotent stem cells from adult human fibroblasts by defined factors. *Cell* *131*, 861–872.
- Vodyanik, M.A., Yu, J., Zhang, X., Tian, S., Stewart, R., Thomson, J.A., and Slukvin, I.I. (2010). A mesoderm-derived precursor for mesenchymal stem and endothelial cells. *Cell Stem Cell* *7*, 718–729.
- Wakitani, S., Goto, T., Pineda, S.J., Young, R.G., Mansour, J.M., Caplan, A.I., and Goldberg, V.M. (1994). Mesenchymal cell-based repair of large, full-thickness defects of articular cartilage. *J. Bone Joint Surg. Am.* *76*, 579–592.
- Wang, T., Chen, K., Zeng, X., Yang, J., Wu, Y., Shi, X., Qin, B., Zeng, L., Esteban, M.A., Pan, G., et al. (2011). The histone demethylases Jhdm1a/1b enhance somatic cell reprogramming in a vitamin-C-dependent manner. *Cell Stem Cell* *9*, 575–587.
- Watanabe, K., Ueno, M., Kamiya, D., Nishiyama, A., Matsumura, M., Wataya, T., Takahashi, J.B., Nishikawa, S., Nishikawa, S., Murguruma, K., et al. (2007). A ROCK inhibitor permits survival of dissociated human embryonic stem cells. *Nat. Biotechnol.* *25*, 681–686.
- Worthley, D.L., Churchill, M., Compton, J.T., Taylor, Y., Rao, M., Si, Y., Levin, D., Schwartz, M.G., Uygur, A., Hayakawa, Y., et al. (2015). Gremlin 1 identifies a skeletal stem cell with bone, cartilage, and reticular stromal potential. *Cell* *160*, 269–284.
- Ye, L., Fan, Z., Yu, B., Chang, J., Al Hezaimi, K., Zhou, X., Park, N.H., and Wang, C.Y. (2012). Histone demethylases KDM4B and KDM6B promotes osteogenic differentiation of human MSCs. *Cell Stem Cell* *11*, 50–61.
- Zhang, W., Li, J., Suzuki, K., Qu, J., Wang, P., Zhou, J., Liu, X., Ren, R., Xu, X., Ocampo, A., et al. (2015). Aging stem cells. A Werner syndrome stem cell model unveils heterochromatin alterations as a driver of human aging. *Science* *348*, 1160–1163.